diabetes dampens the regulation of the clock genes. However, it remains to be elucidated whether the expression of clock genes exhibits rhythmicity and whether clock genes play a role in adipose tissue. To address these issues, we investigated 24-h changes in the mRNA levels of the clock genes and adipocytokines in C57BL/6J mouse adipose tissue. Moreover, we examined whether obesity linked to insulin resistance and type 2 diabetes alters the daily rhythms of the mRNA expression, using KK and KK-A^y mice, which are models of mild and severe, spontaneous obese diabetes, respectively.

Materials and Methods

Mice

In a preliminary study, we found that the mRNA levels of adiponectin and resistin exhibited 24-h rhythmicity in female, but not male, C57BL/6J mice (data not shown). Therefore, only female mice were used in this study. C57BL/6J (Charles River Japan, Yokohama, Japan), KK/Ta, and KK-A^y/Ta mice (CLEA Japan, Tokyo, Japan) were obtained at 8 wk of age and maintained under a specific pathogen-free condition with controlled temperature and humidity and a 12-h light (0700–1900 h), 12-h dark (1900–0700 h) cycle. Mice were housed individually and given a standard laboratory diet (CE-2; CLEA Japan) and water *ad libitum*. Half of the KK and KK-A^y mice were fed CE-2 with 0.02% pioglitazone. After 2 wk, animals were killed to obtain blood, liver, and perigonadal fat samples at the following zeitgeber times (ZTs): 0, 6, 12, and 18, in which ZT 0 is defined as lights on and ZT 12 as lights off. All animal procedures were preformed in accordance with the Guidelines for Animal Research at the Jichi Medical School, Japan.

Measurement of circulating glucose and insulin concentrations

The blood glucose concentration was measured using a Glutest Ace R (Sanwa Kagaku Kenkyusyo, Nagoya, Japan). The RIA for serum insulin was performed using kits purchased from Linco Research (St. Charles, MO). The intra- and interassay coefficients of variation were less than 10%.

RNA extraction and real-time quantitative PCR

The isolation of total RNA was achieved using the RNeasy lipid tissue minikit or the RNeasy minikit according to the manufacturer's instructions (QIAGEN, Valencia, CA). Reverse transcription was performed with 1.2 μg total RNA, random hexamer primer, and RevertAid M-MuLV reverse transcriptase (Fermentas, Hanover, MD). The gene expression was analyzed by real-time quantitative PCR, performed with the ABI Prism 7700 sequence detection system (Applied Biosystems, Foster City, CA), as previously described (22, 23). All specific sets of primers and TaqMan probes were obtained from Applied Biosystems [TaqMan gene expression assays and TaqMan rodent glyceraldehyde-3-phosphate dehydrogenase (GAPDH) control reagents]. The GenBank accession codes were NM_016974 for Dbp, NM_011065 for Per1, NM_011066 for Per2, NM_007489 for Bmal1, NM_007771 for Cry1, NM_009963 for Cry2, NM_009605 for adiponectin, NM_022984 for resistin, NM_021524 for visfatin, and NM_008493 for leptin. All of the primer sets, except for the TaqMan rodent GAPDH control reagents, were designed to be located in two exons to avoid the amplification of potentially contaminating genomic DNA. To control the variation in the amount of DNA available for PCR in the different samples, the gene expression of the target sequence was normalized in relation to the expression of an endogenous control, GAPDH. The data were analyzed using the comparative threshold cycle method because the efficiency of the target amplification was approximately equal to that of the GAPDH amplification (24).

Statistical analysis

Data were analyzed using an ANOVA with a *post hoc* test of Fisher's protected least significant differences (PLSD). The values are presented as the means ± SEM, and $P < 0.05$ was considered significant. All calculations were performed using StatView (version 5.0; SAS Institute, Cary, NC).

Results and Discussion

Rhythmic mRNA expression of clock genes and adipocytokines in visceral adipose tissue of C57BL/6J mice

To investigate whether the mRNA expression of clock genes and adipocytokines shows daily rhythms in visceral adipose tissue, perigonadal fat samples were obtained from 10-wk-old C57BL/6J mice every 6 h throughout a single 24-h period. As shown in Fig. 1, A and B, all clock genes examined (Dbp, Per1, Per2, Bmal1, Cry1, and Cry2) exhibited 24-h rhythmicity ($F = 6.6–32.6$, each $P < 0.01$, one-way ANOVA to test rhythmicity of each gene). In a manner that was consistent with previous observations (10–12, 25) in other peripheral tissues, including the heart, liver, spleen, and kidney, the transcript levels of Dbp, Per1, and Per2 peaked in the latter half of the light phase. On the other hand, the Bmal1 mRNA dropped to near trough levels at the same time. Additionally, the Cry1 and Cry2 mRNA levels peaked at ZT 18 and 12, respectively. These results suggest that an intracellular circadian clock system operates in the visceral adipose tissue as well as in other peripheral tissues.

Because clock genes may also regulate the transcriptional activities of various genes in adipocytes, we further determined the daily mRNA expression profiles of adipocytokines (adiponectin, resistin, visfatin, and leptin). Adiponectin improves insulin sensitivity and prevents atherosclerosis (13), whereas resistin induces insulin resistance in mice (26). Visfatin is a newly identified adipocytokine that can exert insulin-mimetic effects by activating the insulin receptor (27). Leptin is thought to regulate energy homeostasis by stimulating coordinated changes in energy intake and expenditure (14, 18). The mRNA expression of adiponectin showed a significant 24-h rhythm ($F = 4.5$, $P < 0.05$, one-way ANOVA; Fig. 1C) with a peak at ZT 12 and a trough at ZT 0. Interestingly, the profile of resistin ($F = 3.9$, $P < 0.05$) was similar to that of adiponectin, even though resistin counteracts the action of adiponectin. Moreover, the visfatin transcript level also peaked at ZT 12 and dropped to a near trough level by ZT 24 (ZT 0; $F = 6.7$, $P < 0.01$). Furthermore, the leptin mRNA expression tended to exhibit a 24-h rhythm ($F = 2.9$, $P = 0.07$) with a peak in the dark phase. Thus, these results demonstrate that the expression of some adipocytokines is regulated in a time-dependent manner, at least at the mRNA level, although the precise molecular mechanisms underlying these regulations are unknown.

Alterations in the daily mRNA expression profiles of clock genes and adipocytokines in the visceral adipose tissue of obese diabetic mice

In the last decade, it has become evident that various adipocytokines are closely associated with the development of type 2 diabetes, metabolic syndrome, and/or atherosclerosis (13, 14). The plasma concentrations of several adipocytokines, including adiponectin and leptin, have been correlated with visceral fat accumulation (13, 14, 18–20). Moreover, obesity blunts the diurnal rhythm of plasma adi-

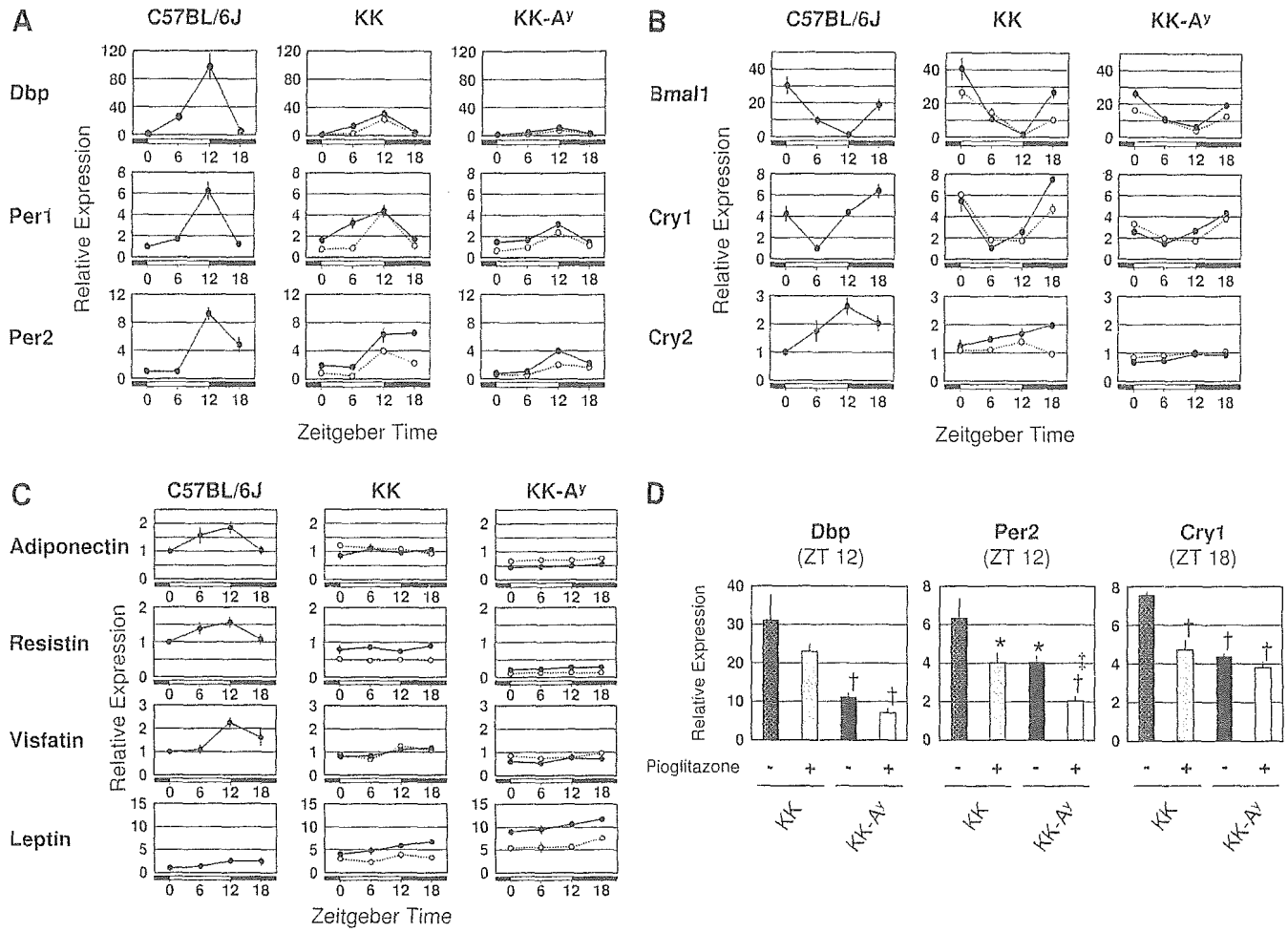

FIG. 1. Daily mRNA expression profiles of the clock genes (A and B) and adipocytokines (C) in the visceral adipose tissues of C57BL/6J, KK, and KK-A^y mice. Female mice were maintained under a 12-h light, 12-h dark cycle and fed a standard diet with (○—○) or without (●—●) 0.02% pioglitazone for 2 wk. Thereafter, perigonadal fat samples were obtained at ZT 0, 6, 12, and 18. Transcript levels of the target genes were determined by real-time quantitative RT-PCR. D, mRNA levels of the representative gene (Dbp, Per2, or Cry1) at the time that its level peaked in C57BL/6J mice were compared among groups using an ANOVA with a *post hoc* test of Fisher's PLSD. All data are means and SEM of five mice at each time point and are expressed as relative values to the lowest values in C57BL/6J mice for each gene. *, $P < 0.05$; †, $P < 0.01$ *vs.* untreated KK mice; ‡, $P < 0.05$ *vs.* untreated KK-A^y mice.

ponectin concentration (19, 20). Thus, it can be speculated that obesity may affect not only adipocytokine but also clock gene expression. To verify this hypothesis, we investigated the daily profiles of mRNA levels for the clock genes and adipocytokines in perigonadal fat of 10-wk-old KK and KK-A^y mice. The KK strain models mild, obese diabetes, whereas the introduction of the A^y allele (KK-A^y) exacerbates the pathophysiological condition with consequent overt diabetes (28). As shown in Table 1, KK mice were significantly heavier than C57BL/6J mice, and obesity was more severe in KK-A^y mice. In addition, obvious hyperglycemia and hyperinsulinemia were detected in KK-A^y but not in KK mice.

In the visceral adipose tissues of both strains and in C57BL/6J mice, all investigated clock genes showed significant rhythmicity (Fig. 1, A and B; $F = 4.0–61.7$, $P < 0.05$ for Cry2 in KK mice, $P < 0.01$ for the other cases, one-way ANOVA). Moreover, the phases of the daily expression rhythms did not differ among the strains in most of the clock genes. Interestingly, their peaks were significantly attenuated in KK-A^y mice, compared with KK mice (Fig. 1, A, B, and D). In addition, the peak level of Dbp, a first-order clock controlled gene, in KK mice was much lower than in C57BL/6J mice ($P < 0.01$, Fisher's PLSD). Therefore, obesity and/or type 2 diabetes appear to affect the intracellular clock system in visceral adipose tissue.

With regard to the daily profiles of adipocytokine mRNAs (Fig. 1C), the rhythmic expression of adiponectin and resistin was not detected in either KK or KK-A^y mice. Additionally, in agreement with previous results (14), the peak levels of adiponectin and resistin were significantly lower (each $P < 0.01$, Fisher's PLSD) in KK mice than in the C57BL/6J mice, and their levels were even lower in KK-A^y mice than KK mice ($P < 0.05$ for adiponectin and $P < 0.01$ for resistin). The visfatin mRNA levels were also lower in KK and KK-A^y mice than in C57BL6J mice (each $P < 0.01$), which is contrary to the previous observations in male KK-A^y mice (27). Because a recent study has reported that the visfatin transcript level is not associated with obesity/metabolic syndrome in rats (29), further studies are needed to elucidate how obesity affects visfatin gene expression in rodents. Unlike adiponec-

TABLE 1. Biological characteristics of female C57BL/6J, KK, and KK-A^y mice after being fed a regular diet with or without 0.02% pioglitazone for 2 wk

Groups	*n* (*n* at each time point)	Body weight (g)	Blood glucose (mg/dl)				Serum insulin (ng/ml)			
			ZT0	ZT6	ZT12	ZT18	ZT0	ZT6	ZT12	ZT18
C57BL/6J										
Untreated	20 (5)	19.9 ± 0.2	153 ± 8	186 ± 26	136 ± 12	155 ± 6	0.2 ± 0.1	0.3 ± 0.1	0.3 ± 0.1	1.1 ± 0.4
KK										
Untreated	20 (5)	29.1 ± 0.3^a	188 ± 8	199 ± 9	185 ± 12	200 ± 12	0.7 ± 0.0	0.7 ± 0.2	0.8 ± 0.2	2.3 ± 0.5
Pioglitazone treated	20 (5)	30.5 ± 0.3^{a,b}	191 ± 9	178 ± 13	149 ± 6	167 ± 9	0.9 ± 0.3	1.0 ± 0.2	0.5 ± 0.1	1.3 ± 0.4
KK-A^y										
Untreated	20 (5)	43.1 ± 0.3^{a,c}	370 ± 54^{a,c}	327 ± 34^{a,c}	348 ± 43^{a,c}	425 ± 29^{a,c}	33.7 ± 13.0^{a,c}	27.2 ± 9.6^{a,c}	12.6 ± 2.8^{a,c}	22.4 ± 1.8^{a,d}
Pioglitazone treated	20 (5)	46.6 ± 0.4^{a,b,c}	183 ± 18^b	219 ± 5^b	189 ± 6^b	185 ± 24^b	16.2 ± 6.0	6.7 ± 2.6^b	5.3 ± 0.9^{b,d,e}	24.0 ± 11.2^{a,c}

Data are means ± SEM.
[a] $P < 0.01$ *vs.* C57BL/6J.
[b] $P < 0.01$ *vs.* untreated mice.
[c] $P < 0.01$ *vs.* untreated KK.
[d] $P < 0.05$ vs. untreated KK.
[e] $P < 0.05$ *vs.* C57BL/6J.

tin and resistin, visfatin still showed mild rhythmicity in KK and KK-A^y mice ($F = 4.2$ and 5.1, respectively, each $P < 0.05$, one-way ANOVA). Its transcript levels in both strains as well as C57BL/6J mice rose at ZT 6, remained at higher levels during the first half of the dark phase, and dropped to near trough levels by ZT 24. Moreover, leptin exhibited daily rhythms with a peak at ZT 18 and a trough at ZT 0 in KK ($F = 3.4$, $P < 0.05$) and KK-A^y mice ($F = 3.9$, $P < 0.05$). Thus, the daily mRNA expression rhythms of adipocytokines do not seem to be equally affected by obesity and/or type 2 diabetes. These results suggest that not only clock genes but also some other factors influence the diurnal variations in the transcript levels of adipocytokines to varying degrees.

Effects of pioglitazone on the daily mRNA expression profiles of clock genes and adipocytokines in the visceral adipose tissue of obese diabetic mice

Recent studies have suggested that thiazolidinediones, a class of oral antidiabetic agents, act as insulin sensitizers by at least partly regulating the expression of adipocytokines (14, 30). Therefore, we speculated that thiazolidinediones might correct the daily mRNA expression rhythms of clock genes and adipocytokines in obese diabetic mice. As shown in Table 1, a 2-wk treatment with pioglitazone significantly decreased both circulating glucose and insulin concentrations in KK-A^y mice. Pioglitazone treatment also affected the daily profiles of all investigated clock genes, except Cry1, in both KK and KK-A^y mice (Fig. 1, A and B; $F = 7.6–46.2$, each $P < 0.01$, two-way ANOVA). However, contrary to our expectations, pioglitazone did not improve, but rather worsened, the peak levels of the clock genes, which were diminished in association with obesity/type 2 diabetes (Fig. 1, A, B, and D). Moreover, the rhythmic mRNA expression of leptin detected in untreated mice disappeared in both pioglitazone-treated groups (Fig. 1C). Furthermore, visfatin, adiponectin, and resistin did not show any daily rhythmicity in pioglitazone-treated KK-A^y mice. On the other hand, as previously reported (14, 30), pioglitazone significantly increased the mRNA levels of adiponectin and decreased those of resistin and leptin in KK-A^y mice (Fig. 1C; $F = 24.8$, 60.6 and 82.9, respectively, each $P < 0.01$, two-way ANOVA). In addition, this treatment also increased visfatin levels ($F = 24.3$, $P < 0.01$). Thus, pioglitazone affected the gene expression levels of adipocytokines without the improvement of the clock gene system. These results support the view that some other factors, as well as clock genes, regulate the daily rhythms in mRNA levels for adipocytokines.

Effects of type 2 diabetes and pioglitazone on the daily mRNA expression profiles of clock genes in the liver

To elucidate whether the above-mentioned findings are specific to the visceral adipose tissue, we further determined daily mRNA expression profiles of the clock genes in the liver (Fig. 2). Consistent with the effect detected in the adipose tissue, overt obesity/type 2 diabetes significantly dampened the peaks of all investigated clock genes. On the other hand, mild obesity might not affect the clock gene system because the peak levels of clock genes in KK mice were not lower than those in C57BL/6J mice. Interestingly, contrary to the findings in the adipose tissue, pioglitazone treatment improved

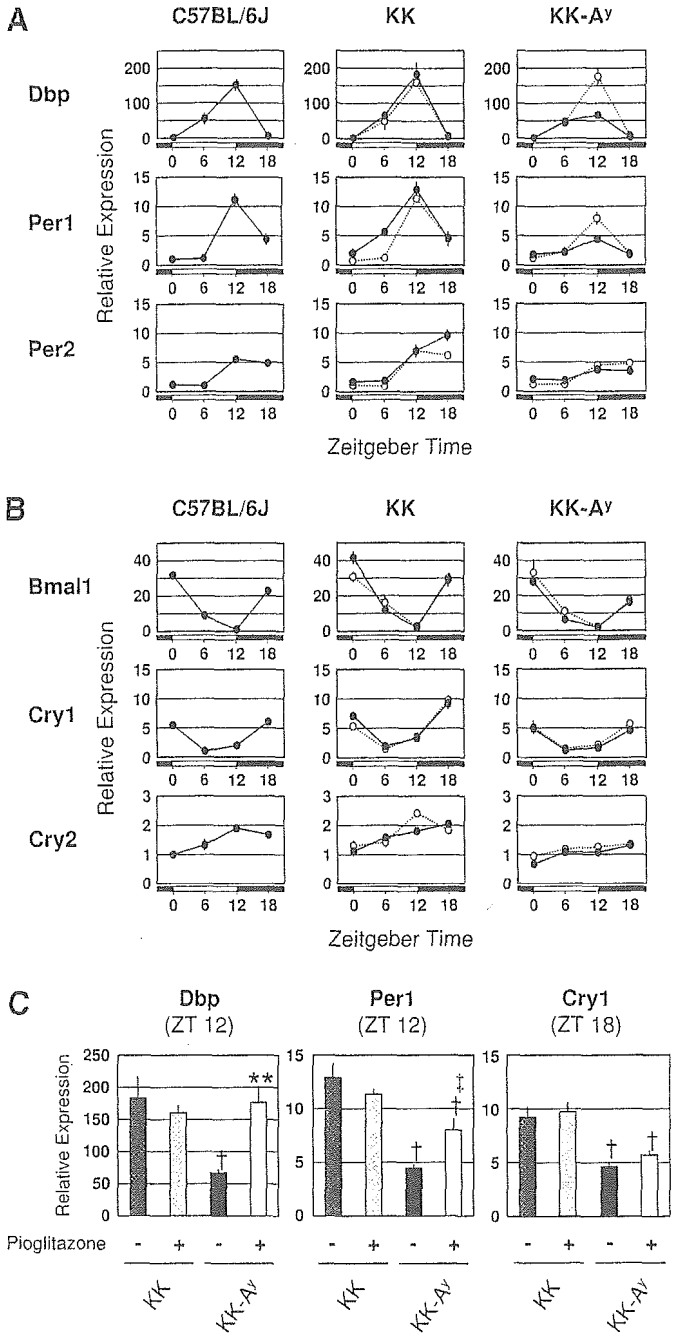

FIG. 2. A and B, Daily mRNA expression profiles of the clock genes in the liver of C57BL/6J, KK, and KK-A^y mice after being fed a regular diet with (○—○) or without (●—●) pioglitazone for 2 wk. C, mRNA levels of the representative gene (Dbp, Per1, or Cry1) at the time when its level peaked in C57BL/6J mice were compared among groups using an ANOVA with a *post hoc* test of Fisher's PLSD. All data are means and SEM of four mice at each time point and are expressed as relative values to the lowest values in C57BL/6J mice for each gene. †, $P < 0.01$ *vs.* untreated KK mice; ‡, $P < 0.05$; **, $P < 0.01$ *vs.* untreated KK-A^y mice.

the rhythmicity of the mRNA expression of the clock genes in KK-A^y mice. These results further support the view that pathophysiological condition of obese type 2 diabetes is related to the impaired clock gene system in peripheral tissues.

Peroxisome proliferators-activated receptor (PPAR)-γ is a nuclear receptor that regulates various biological processes such as differentiation, proliferation, metabolism, and maintenance of insulin sensitivity (31). It has been recently shown that PPARγ can directly regulate the transcription of the clock gene Rev-Erbα (32). Increasing Rev-Erbα protein acts to repress Bmal1 transcription in the clock gene system (2, 3). Because pioglitazone is a PPARγ agonist, treatment with the agent may directly affect the transcription of Rev-Erbα. In the present study, pioglitazone attenuated the rhythmicity of the clock gene expression in the adipose tissue but improved that in the liver. The expression of PPARγ is known to be considerably higher in adipose than in most other tissues, including liver (31, 33). Therefore, it is possible that pioglitazone mainly exerted direct effects on the clock gene system in the adipose tissue, whereas pioglitazone might ameliorate the attenuated rhythmicity of the clock genes in the liver via indirect effects, such as the improvement of hyperglycemia and/or hyperinsulinemia. The impaired rhythmicity of the mRNA expression of the clock genes and adipocytokines in the adipose tissue did not seem to affect the rhythmicity in the liver.

Turek *et al.* (34) recently reported that homozygous Clock mutant mice are hyperphagic and obese and that they develop a metabolic syndrome of hyperleptinemia, hyperglycemia, and hyperlipidemia. The Clock mutant mice have a severely disturbed diurnal feeding rhythm accompanying the attenuated mRNA expression of hypothalamic peptides involved in energy balance. In contrast, neither obese diabetes nor pioglitazone treatment affected the daily feeding rhythms of mice in our study (Fig. 3), although feeding is a dominant zeitgeber (timing cue) for peripheral clocks (21, 35, 36). Therefore, it is still possible that obesity, namely adipocyte hypertrophy, directly causes the alteration of the circadian clock system in adipose tissue, even if the central clock system is affected in obese diabetic mice. Actually, BMAL1 has been recently shown to play essential roles in the regulation of adipocyte differentiation and lipogenesis (37). The Rev-Erbα also promotes PPARγ-induced adipocyte differentiation (32). Moreover, inactivation of BMAL1 or CLOCK suppresses the diurnal variation in glucose and triglycerides and abolishes gluconeogenesis in mice (38). Thus, the clock gene system appears to be involved in the development of type 2 diabetes at least via the regulation of adipocyte differentiation and gluconeogenesis.

The rhythmicity of clock gene expression might be important

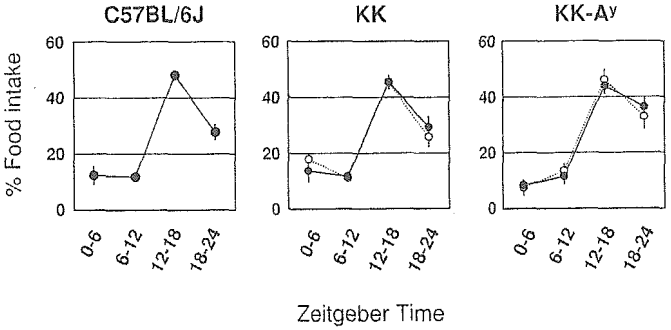

FIG. 3. Daily profiles of food intake in C57BL/6J, KK, and KK-A^y mice after being fed a regular diet with (○—○) or without (●—●) pioglitazone for 2 wk. Data are means ± SEM of five mice in each group and are expressed as percentages of total food intake.

to preservation of health. Because the Per2 gene exerts a tumor-suppressive effect by regulating DNA damage-responsive pathways (39), attenuated expression of the clock genes might cause not only type 2 diabetes but also cancer. Our results suggest that various factors, including obesity/diabetes, pioglitazone, and sex, could affect the rhythmic expression of the clock genes in peripheral tissues. Whether the control of clock gene system prevents the development of type 2 diabetes or cancer remains to be determined.

In conclusion, we found that mRNA expression of the clock genes and adipocytokines shows significant 24-h rhythmicity in mouse visceral adipose tissue. Moreover, spontaneous obese diabetes attenuated this rhythmic expression in most of the clock and adipocytokine genes investigated. Likewise, obese diabetes impaired the rhythmic expression of the clock genes in the liver. Interestingly, pioglitazone treatment improved the attenuated rhythmicity in the liver but not the adipose tissue. Further studies are needed to clarify whether impairment of the clock gene system in visceral adipose tissue and liver is involved in the development of type 2 diabetes and/or metabolic syndrome.

Acknowledgments

Received June 24, 2005. Accepted September 8, 2005.

Address all correspondence and requests for reprints to: Dr. Akio Fujimura, Department of Pharmacology, Jichi Medical School, Tochigi 329-0498, Japan. E-mail: akiofuji@jichi.ac.jp.

References

1. Ripperger JA, Schibler U 2001 Circadian regulation of gene expression in animals. Curr Opin Cell Biol 13:357–362
2. Reppert SM, Weaver DR 2002 Coordination of circadian timing in mammals. Nature 418:935–941
3. Lowrey PL, Takahashi JS 2004 Mammalian circadian biology: elucidating genome-wide levels of temporal organization. Annu Rev Genomics Hum Genet 5:407–441
4. Gekakis N, Staknis D, Nguyen HB, Davis FC, Wilsbacher LD, King DP, Takahashi JS, Weitz CJ 1998 Role of the CLOCK protein in the mammalian circadian mechanism. Science 280:1564–1569
5. Bunger MK, Wilsbacher LD, Moran SM, Clendenin C, Radcliffe LA, Hogenesch JB, Simon MC, Takahashi JS, Bradfield CA 2000 Mop3 is an essential component of the master circadian pacemaker in mammals. Cell 103:1009–1017
6. Kume K, Zylka MJ, Sriram S, Shearman LP, Weaver DR, Jin X, Maywood ES, Hastings MH, Reppert SM 1999 mCRY1 and mCRY2 are essential components of the negative limb of the circadian clock feedback loop. Cell 98:193–205
7. Vitaterna MH, Selby CP, Todo T, Niwa H, Thompson C, Fruechte EM, Hitomi K, Thresher RJ, Ishikawa T, Miyazaki J, Takahashi JS, Sancar A 1999 Differential regulation of mammalian period genes and circadian rhythmicity by cryptochromes 1 and 2. Proc Natl Acad Sci USA 96:12114–12119
8. Okamura H, Miyake S, Sumi Y, Yamaguchi S, Yasui A, Muijtjens M, Hoeijmakers JH, van der Horst GT 1999 Photic induction of mPer1 and mPer2 in cry-deficient mice lacking a biological clock. Science 286:2531–2534
9. Shearman LP, Sriram S, Weaver DR, Maywood ES, Chaves I, Zheng B, Kume K, Lee CC, van der Horst GT, Hastings MH, Reppert SM 2000 Interacting molecular loops in the mammalian circadian clock. Science 288:1013–1019
10. Panda S, Antoch MP, Miller BH, Su AI, Schook AB, Straume M, Schultz PG, Kay SA, Takahashi JS, Hogenesch JB 2002 Coordinated transcription of key pathways in the mouse by the circadian clock. Cell 109:307–320
11. Storch KF, Lipan O, Leykin I, Viswanathan N, Davis FC, Wong WH, Weitz CJ 2002 Extensive and divergent circadian gene expression in liver and heart. Nature 417:78–83
12. Yoo SH, Yamazaki S, Lowrey PL, Shimomura K, Ko CH, Buhr ED, Siepka SM, Hong HK, Oh WJ, Yoo OJ, Menaker M, Takahashi JS 2004 PERIOD2::LUCIFERASE real-time reporting of circadian dynamics reveals persistent circadian oscillations in mouse peripheral tissues. Proc Natl Acad Sci USA 101:5339–5346
13. Matsuzawa Y, Funahashi T, Kihara S, Shimomura I 2004 Adiponectin and metabolic syndrome. Arterioscler Thromb Vasc Biol 24:29–33
14. Fasshauer M, Paschke R 2003 Regulation of adipocytokines and insulin resistance. Diabetologia 46:1594–1603
15. Saladin R, De Vos P, Guerre-Millo M, Leturque A, Girard J, Staels B, Auwerx J 1995 Transient increase in obese gene expression after food intake or insulin administration. Nature 377:527–529
16. Pickavance L, Tadayyon M, Williams G, Vernon RG 1998 Lactation suppresses diurnal rhythm of serum leptin. Biochem Biophys Res Commun 248:196–199
17. Ahrén B 2000 Diurnal variation in circulating leptin is dependent on gender, food intake and circulating insulin in mice. Acta Physiol Scand 169:325–331
18. Sinha MK, Ohannesian JP, Heiman ML, Kriauciunas A, Stephens TW, Magosin S, Marco C, Caro JF 1996 Nocturnal rise of leptin in lean, obese, and non-insulin-dependent diabetes mellitus subjects. J Clin Invest 97:1344–1347
19. Calvani M, Scarfone A, Granato L, Mora EV, Nanni G, Castagneto M, Greco AV, Manco M, Mingrone G 2004 Restoration of adiponectin pulsatility in severely obese subjects after weight loss. Diabetes 53:939–947
20. Yildiz BO, Suchard MA, Wong ML, McCann SM, Licinio J 2004 Alterations in the dynamics of circulating ghrelin, adiponectin, and leptin in human obesity. Proc Natl Acad Sci USA 101:10434–10439
21. Kudo T, Akiyama M, Kuriyama K, Sudo M, Moriya T, Shibata S 2004 Night-time restricted feeding normalises clock genes and Pai-1 gene expression in the db/db mouse liver. Diabetologia 47:1425–1436
22. Ando H, Tsuruoka S, Yamamoto H, Takamura T, Kaneko S, Fujimura A 2004 Effects of pravastatin on the expression of ATP-binding cassette transporter A1. J Pharmacol Exp Ther 311:420–425
23. Ando H, Tsuruoka S, Yamamoto H, Takamura T, Kaneko S, Fujimura A 2005 Regulation of cholesterol 7α-hydroxylase mRNA expression in C57BL/6 mice fed an atherogenic diet. Atherosclerosis 178:265–269
24. Su YR, Linton MF, Fazio S 2002 Rapid quantification of murine ABC mRNAs by real time reverse transcriptase-polymerase chain reaction. J Lipid Res 43:2180–2187
25. Yamamoto T, Nakahata Y, Soma H, Akashi M, Mamine T, Takumi T 2004 Transcriptional oscillation of canonical clock genes in mouse peripheral tissues. BMC Mol Biol 5:18
26. Steppan CM, Bailey ST, Bhat S, Brown EJ, Banerjee RR, Wright CM, Patel HR, Ahima RS, Lazar MA 2001 The hormone resistin links obesity to diabetes. Nature 409:307–312
27. Fukuhara A, Matsuda M, Nishizawa M, Segawa K, Tanaka M, Kishimoto K, Matsuki Y, Murakami M, Ichisaka T, Murakami H, Watanabe E, Takagi T, Akiyoshi M, Ohtsubo T, Kihara S, Yamashita S, Makishima M, Funahashi T, Yamanaka S, Hiramatsu R, Matsuzawa Y, Shimomura I 2005 Visfatin: a protein secreted by visceral fat that mimics the effects of insulin. Science 307:426–430
28. Suto J, Matsuura S, Imamura K, Yamanaka H, Sekikawa K 1998 Genetic analysis of non-insulin-dependent diabetes mellitus in KK and KK-Ay mice. Eur J Endocrinol 139:654–661
29. Kloting N, Kloting I 2005 Visfatin: gene expression in isolated adipocytes and sequence analysis in obese WOKW rats compared with lean control rats. Biochem Biophys Res Commun 332:1070–1072
30. Arner P 2003 The adipocyte in insulin resistance: key molecules and the impact of the thiazolidinediones. Trends Endocrinol Metab 14:137–145
31. Rosen ED, Spiegelman BM 2001 PPARγ: a nuclear regulator of metabolism, differentiation, and cell growth. J Biol Chem 276:37731–37734
32. Fontaine C, Dubois G, Duguay Y, Helledie T, Vu-Dac N, Gervois P, Soncin F, Mandrup S, Fruchart JC, Fruchart-Najib J, Staels B 2003 The orphan nuclear receptor Rev-Erbα is a peroxisome proliferators-activated receptor (PPAR) γ target gene and promotes PPARγ-induced adipocyte differentiation. J Biol Chem 278:37672–37680
33. Chawla A, Schwarz EJ, Dimaculangan DD, Lazar MA 1994 Peroxisome proliferators-activated receptor (PPAR) γ: Adipose-predominant expression and induction early in adipocyte differentiation. Endocrinology 135:798–800
34. Turek FW, Joshu C, Kohsaka A, Lin E, Ivanova G, McDearmon E, Laposky A, Losee-Olson S, Easton A, Jensen DR, Eckel RH, Takahashi JS, Bass J 2005 Obesity and metabolic syndrome in circadian Clock mutant mice. Science 308:1043–1045
35. Schibler U, Ripperger J, Brown SA 2003 Peripheral circadian oscillators in mammals: time and food. J Biol Rhythms 18:250–260
36. Kobayashi H, Oishi K, Hanai S, Ishida N 2004 Effect of feeding on peripheral circadian rhythms and behaviour in mammals. Genes Cells 9:857–864
37. Shimba S, Ishii N, Ohta Y, Ohno T, Watabe Y, Hayashi M, Wada T, Aoyagi T, Tezuka M 2005 Brain and muscle Arnt-like protein-1 (BMAL1), a component of the molecular clock, regulates adipogenesis. Proc Natl Acad Sci USA 102:12071–12076
38. Rudic RD, McNamara P, Curtis AM, Boston RC, Panda S, Hogenesch JB, FitzGerald GA 2004 BMAL1 and CLOCK, two essential components of the circadian clock, are involved in glucose homeostasis. PLoS Biol 2:e377
39. Fu L, Pelicano H, Liu J, Huang P, Lee CC 2002 The circadian gene Period2 plays an important role in tumor suppression and DNA damage response *in vivo*. Cell 111:41–50

DOI:10.1111/j.1365-2125.2005.02462.x

Effects of grapefruit juice on the pharmacokinetics of pitavastatin and atorvastatin

Hitoshi Ando,[1] Shuichi Tsuruoka,[1] Hayato Yanagihara,[1] Koh-ichi Sugimoto,[1] Masaaki Miyata,[2] Yasushi Yamazoe,[2] Toshinari Takamura,[3] Shuichi Kaneko[3] & Akio Fujimura[1]

[1]Division of Clinical Pharmacology, Department of Pharmacology, Jichi Medical School, Tochigi, Japan, [2]Division of Drug Metabolism and Molecular Toxicology, Graduate School of Pharmaceutical Sciences, Tohoku University, Sendai, Japan and [3]Department of Diabetes and Digestive Disease, Kanazawa University Graduate School of Medical Science, Kanazawa, Japan.

Correspondence
Akio Fujimura, MD, PhD,
Department of Pharmacology, Jichi Medical School, Tochigi 329–0498, Japan.
Tel: + 81 285 58 7388
Fax: + 81 285 44 7562
E-mail: akiofuji@jichi.ac.jp

Keywords
pitavastatin, atorvastatin, HMG-CoA reductase inhibitors, grapefruit juice, CYP3A4, drug interaction

Received
15 February 2005
Accepted
19 May 2005

Aims
To compare the effects of grapefruit juice (GFJ) on the pharmacokinetics of pitavastatin and atorvastatin.

Methods
In a randomized, four-phase crossover study, eight healthy subjects consumed either GFJ or water t.i.d. for 4 days in each trial. On each final day, a single dose of 4 mg pitavastatin or 20 mg atorvastatin was administered.

Results
GFJ increased the mean AUC_{0-24} of atorvastatin acid by 83% (95% CI 23–144%) and that of pitavastatin acid by 13% (−3 to 29%).

Conclusions
Pitavastatin, unlike atorvastatin, appears to be scarcely affected by the CYP3A4-mediated metabolism.

Introduction

Most of the 3-hydroxy-3-methylglutaryl coenzyme A reductase inhibitors (statins) except pravastatin are metabolized by the cytochrome P450 (CYP) enzymes [1]. Interactions involving CYP are therefore possible. For example, itraconazole has been shown to increase the area under the plasma concentration-time curve (AUC) of atorvastatin acid and lactone by 3-fold and 4-fold, respectively [1].

Pitavastatin is a novel synthetic statin, which has a highly potent cholesterol-lowering action similar to that of atorvastatin [2]. The long-term lipid-modifying effects and safety profiles of pitavastatin have already been confirmed in hypercholesterolaemic patients [2].

Pitavastatin acid, which is the major active form, and the inactive lactone form are metabolized to some extent by CYP2C9 and CYP3A4, respectively, in human hepatic microsomes, but the clearance of pitavastatin is very low and only one-thirteenth of atorvastatin clearance [3]. The bioavailabilities of pitavastatin and atorvastatin are 60 and 12%, respectively [2]. Moreover, after the repeated administration of pitavastatin in healthy subjects, its metabolites other than pitavastatin lactone were scarcely detected in plasma [2]. The pharmacokinetics of pitavastatin therefore appear to be hardly affected by the CYP-system modulators, but no direct evidence has been reported clinically. To address this issue, we investigated the effects of a repeated intake of grapefruit juice (GFJ), a potent CYP3A4 inhibitor [1, 4], on the pharmacokinetics of pitavastatin and atorvasatin in healthy subjects.

Methods

This study was performed in an open, randomized, four-phase crossover design with the intervals of 2 weeks. The protocol was approved by the Ethics Committee of Jichi Medical School (Tochigi, Japan).

Eight healthy Japanese men (age, 23–34 years; weight, 60–72 kg) participated after written informed consent. The subjects were instructed not to take any medications, herbal supplements and tea, and any foods or drinks containing component(s) of grapefruits, pomelos, sweet or sour oranges, throughout the study period. Caffeine-containing beverages and smoking were avoided from one night before each study day until after the final blood sampling on the next morning. The subjects consumed 250 mL of single-strength GFJ (Tropicana, Kirin Beverage Co., Tokyo, Japan) or water t.i.d. for 3 days just before each trial according to a randomized schedule. On each study day, they took a single oral dose of 4 mg pitavastatin (two 2-mg Livalo tablets, Kowa Co., Nagoya, Japan) or 20 mg atorvastatin (two 10-mg Lipitor tablets, Yamanouchi Pharmaceutical Co., Tokyo, Japan) with 250 mL of GFJ or water at 08.00 h. The subjects also consumed 250 mL of GFJ or water at 12.00 h and 20.00 h. They had fasted overnight, had a standardized meal at 12.00 h, and were allowed to take supper 12 h after dosing.

On each study day, venous blood was taken immediately before and at 0.5, 1, 2, 3, 4, 6, 8, 12, and 24 h after the administration of pitavastatin or atorvastatin. To prevent photolysis, the plasma samples for the measurement of pitavastatin were harvested into the light-protected tubes, immediately flash-frozen in the dry ice/methanol bath, and then stored at −80 °C until analysis. The samples for the measurement of atorvastatin were stored at −20 °C until use.

Plasma concentrations of pitavastatin acid and lactone, atorvastatin acid and lactone, and 2-hydroxy atorvastatin acid were quantified by the liquid chromatography-mass spectrometry methods. Briefly, 150 μL of internal standard solution containing racemic iprolact (for pitavastatin acid), 2-hydroxy atorvastatin-D5 (for pitavastatin lactone and 2-hydroxy atorvastatin acid), atorvastatin-D5 (for atorvastatin acid), or atorvastatin lactone-D5 (for atorvastatin lactone) was added to 50 μL of plasma. After centrifugation, aliquots were injected onto the HPLC column. Zorbax Extend-C18 columns (50 × 2.1 mm, 3.5 μm) (Agilent Technologies, Palo Alto, CA, USA) were used for analytical separation. The mobile phase consisted of acetonitrile and either 0.1% ammonium hydroxide in water (for pitavastatin compounds) or 10 mM ammonium acetate with 0.4% ammonia hydroxide in water (for atorvastatin compounds). The effluent was delivered to a Sciex 3000 quadrupole mass spectrometer (Applied Biosystems/MDS Sciex, Concord, Canada). The ion transitions monitored were *m/z* 422.3/290.0 for pitavastatin acid, *m/z* 404.0/290.2 for pitavastatin lactone, *m/z* 559.2/440.6 for atorvastatin acid, *m/z* 541.2/448.5 for atorvastatin lactone, and *m/z* 575.3/440.6 for 2-hydroxy atorvastatin acid. The lower quantification limits for pitavastatin and atorvastatin compounds were 0.2 and 0.4 ng mL^{-1}, respectively. The interassay coefficients of variation and accuracy were all ≤ 14.0% and 91.8–110.0%.

The pharmacokinetics were characterized by maximum concentration in plasma (C_{max}), time to maximum plasma concentration (t_{max}), elimination half-life ($t^1/_2$), and AUC between time zero and 24 h after dosing (AUC_{0-24}). The elimination $t^1/_2$ was calculated as $\ln 2/k_e$. The AUC_{0-24} was calculated by the trapezoidal rule.

Furanocoumarins were extracted with ethyl acetate and isolated using the HPLC systems as described previously [4]. We measured in triplicate the following four compounds: bergamottin, 6',7'-dihydroxybergamottin (DHB), 4-[[6-hydroxy-7[[1-[(1-hydroxy-1-methyl) ethyl]-4-methyl-6-(7-oxo-7*H*-furo[3,2-*g*][1]benzopyran-4-yl)-4-hexenyl]oxy]-3,7-dimethyl-2-octenyl]oxy]-7*H*-furo[3,2-*g*][1]benzopyran-7-one (GF-I-1), and 4-[[6-hydroxy-7[[4-methyl-1-(1-methylethenyl)-6-(7-oxo-7*H*-furo[3,2-g][1]benzopyran-4-yl)-4-hexenyl]oxy]-3,7-dimethyl-2-octenyl]oxy]-7*H*-furo[3,2-*g*][1]benzopyran-7-one (GF-I-4).

Data were analysed by the Wilcoxon signed rank test. Values are presented as the means and their 95% confidence intervals (CI), and a *P*-value of less than 0.05 was considered significant.

Comparative Study of Taste Disturbance by Losartan and Perindopril in Healthy Volunteers

Shuichi Tsuruoka
Michi Wakaumi
Nobutaka Araki
Takashi Ioka
Kohichi Sugimoto
Akio Fujimura

Reprinted from Journal of Clinical Pharmacology
Volume 45, No. 11, November 2005, pp. 1319-1323

Comparative Study of Taste Disturbance by Losartan and Perindopril in Healthy Volunteers

Shuichi Tsuruoka, Michi Wakaumi, Nobutaka Araki, Takashi Ioka, Kohichi Sugimoto, and Akio Fujimura

The aim of this study was to compare the degree of taste disturbance by losartan, an angiotensin II receptor blocker, with that of perindopril, an angiotensin-converting enzyme inhibitor. Perindopril erbumine (2 mg), losartan potassium (25 mg), or vehicle was given to Japanese volunteers (n = 7) for 14 days in a randomized, placebo-controlled, 3-way crossover design with a 14-day washout period. Gustometry by filter-paper test and electrogustometry were performed before and at the end of each trial. Plasma renin activity (PRA) and serum and salivary zinc concentrations were measured. One subject dropped out because of a perindopril-induced dry cough, but no one claimed a taste disturbance. Detection thresholds of 4 basic tastes (sweet, salty, sour, and bitter) by the paper-disc test and electrogustometry were significantly worsened, and plasma renin activity was elevated by the drugs, whereas the deteriorating effects of 2 drugs did not significantly differ. These drugs did not affect zinc concentrations in plasma and saliva. It was concluded that losartan and perindopril similarly alter taste sensitivity during repeated dosing of the drugs.

Keywords: *Dysgeusia; angiotensin-converting enzyme inhibitor; angiotensin II receptor blockers; adverse drug reactions; gustometry*

Journal of Clinical Pharmacology, 2005;45:1319-1323

Several endogenous and exogenous factors cause taste disturbances, about 20% of which are drug related.[1] Captopril, an angiotensin-converting enzyme (ACE) inhibitor, especially induces taste disturbance because thiol-radical(-SH) within the compound can chelate with serum zinc, and the depletion of zinc subsequently leads to taste disturbance.[1-3] However, other ACE inhibitors without thiol-radical are also reported to cause this event by unknown mechanisms.[2] With perindopril, an ACE inhibitor, 1 case of drug-related taste disturbance has been reported.[2] Cases of dysgeusia or ageusia have also been reported in patients treated with some angiotensin II receptor blockers (ARBs) such as losartan.[4,5] We have recently showed that taste sensitivity was subclinically disturbed by candesartan in healthy volunteers.[6]

From the Department of Pharmacology, Division of Clinical Pharmacology, Jichi Medical School, Tochigi, Japan. Shuichi Tsuruoka and Michi Wakaumi contributed equally to the manuscript. Submitted for publication June 21, 2005; revised version accepted July 13, 2005. Address for reprints: Shuichi Tsuruoka, MD, Department of Pharmacology, Division of Clinical Pharmacology, Jichi Medical School, 3311 Yakushiji, Minamikawachi, Kawachi, Tochigi 329-0498, Japan; e-mail: tsuru@jichi.ac.jp.
DOI: 10.1177/0091270005280445

Recently, the effectiveness of coadministration of both ARB and ACE was reported in some clinical situations.[7] The opportunity to prescribe both drugs at the same time may increase in the future. However, it remains uncertain whether quantity and quality of the taste disturbance by ARBs and ACE inhibitors are similar. In this study, we directly compared the effect of the repeated oral dosing of losartan, an ARB, and an ACE inhibitor, perindopril, on taste sensitivity by a randomized, double-blind, placebo-controlled crossover study in healthy volunteers.

METHODS

Study Design

Seven healthy Japanese men (29-46 years) were enrolled in this study. Women, smokers, and subjects younger than age 20 or older than age 50 years were excluded. Demographic characteristics of the subjects are listed in Table I. All subjects gave written informed consent. A randomized, double-blind, placebo-controlled, 3-way crossover design with a washout period of 2 weeks was used in this study.[6] In brief, detection thresholds for tastes were determined and salivary fluid was obtained

Results

Because the amounts of furanocoumarins might depend on the lots of GFJ, their concentrations in each lot used in this study ($n = 3$) were measured. The mean values (ranges) of bergamottin, DHB, GF-I-1, and GF-I-4 concentrations were 21.0 (16.2–24.4), 10.4 (5.2–13.8), 0.50 (0.36–0.59), and 0.59 (0.45–0.70) μM, respectively. These concentrations of GF-I-1 and GF-I-4 can completely inhibit the CYP3A4-mediated oxidations *in vitro* [4]. The differences of furanocoumarin concentrations among the lots were small.

To investigate the effect of GFJ on the pharmacokinetics of atorvastatin, we measured the concentrations of its active acid form, inactive lactone form, and 2-hydroxy atorvastatin acid, one of the major active metabolites, after a single dosing of 20 mg atorvastatin. The formation of atorvastatin metabolites, including 2-hydroxy atorvastatin, is shown to be catalysed by CYP3A4 [5]. GFJ significantly increased the mean AUC_{0-24} of atorvastatin acid by 83% (Table 1), from 21.3 to 39.0 ng mL^{-1} h (95% CI for difference, 4.8–30.7), as reported previously [5, 6]. The AUC_{0-24} were increased in seven of the eight subjects, and the increase ranged from 1.5-fold to 7.1-fold. The increase of C_{max} did not reach to a statistical significance ($P = 0.09$), probably due to small sample size. The AUC_{0-24} and C_{max} of atorvastatin lactone and of 2-hydroxy atorvastatin acid were not significantly altered, whereas the mean t_{max} of 2-hydroxy atorvastatin acid was prolonged from 3.2 to 9.4 h by GFJ.

GFJ increased the mean AUC_{0-24} of pitavastatin acid only by 13%, from 194.2 to 220.1 ng mL^{-1} h (95% CI for difference, −5.0 to 56.9; Table 2). Moreover, the C_{max} remained unchanged. The $t_{1/2}$ and AUC_{0-24} of pitavastatin lactone were significantly increased.

Discussion

GFJ had only a minimal effect on pitavastatin pharmacokinetics, while the expected increased concentrations of atorvastatin were confirmed.

Interestingly, the pharmacokinetic parameters of both atorvastatin and pitavastatin varied widely in the subjects even in the trial with water. For example, the AUC_{0-24} of atorvastatin acid ranged from 4.5 to 43.3 ng mL^{-1} h, and the C_{max} of pitavastatin acid varied from 25.6 to 246.0 ng mL^{-1} in the trial with water. The AUC_{0-24} of atorvastatin acid in the subject who had the highest value in the trial with water did not increase any more in the trial with GFJ. It can thus be speculated that there are great differences in the inherent ability to metabolize the statins among the subjects. Recent studies have revealed that polymorphisms of both CYP enzymes and transporters may influence the cholesterol-

Table 1
The pharmacokinetic parameters of atorvastatin acid, atorvastatin lactone, and 2-hydroxy atorvastatin acid after a single dosing of 20 mg atorvastatin with water or grapefruit juice (mean and 95% confidence interval)

Parameter	Water	GFJ	Difference between water and GFJ	*P*-value
Atorvastatin acid				
C_{max} (ng mL^{-1})	4.2 (2.2, 6.3)	7.2 (2.6, 11.7)	2.9 (−0.2, 6.1)	0.09
t_{max} (h)	1.4 (0.4, 2.4)	1.4 (0.8, 2.0)	−0.1 (−1.0, 0.9)	0.92
AUC_{0-24} (ng mL^{-1} h)	21.3 (10.6, 32.0)	39.0 (24.4, 53.7)	17.7 (4.8, 30.7)	<0.05
Atorvastatin lactone				
C_{max} (ng mL^{-1})	2.1 (0.8, 3.5)	3.5 (1.7, 5.2)	1.3 (−0.3, 3.0)	0.12
t_{max} (h)	6.1 (2.4, 9.9)	3.3 (1.2, 5.3)	−2.9 (−6.8, 1.0)	0.13
AUC_{0-24} (ng mL^{-1} h)	25.6 (3.9, 47.2)	41.1 (17.8, 64.5)	15.6 (−2.3, 33.4)	0.07
2-hydroxy atorvastatin acid				
C_{max} (ng mL^{-1})	3.6 (1.1, 6.1)	2.0 (1.1, 2.9)	−1.6 (−4.1, 0.8	0.12
t_{max} (h)	3.2 (0.0, 6.4)	9.4 (6.2, 12.5)	6.2 (2.5, 9.9)	<0.05
AUC_{0-24} (ng mL^{-1} h)	28.6 (18.6, 38.7)	29.5 (18.3, 40.5)	0.8 (−7.4, 9.0)	0.78

GFJ, Grapefruit juice; C_{max}, maximum concentration in plasma; t_{max}, time to maximum plasma concentration; AUC_{0-24}, area under the plasma concentration – time curve between time zero and 24 h after dosing.

Table 2
The pharmacokinetic parameters of pitavastatin acid and pitavastatin lactone after a single dosing of 4 mg pitavastatin with water or grapefruit juice (mean and 95% confidence interval)

Parameter	Water	GFJ	Difference between water and GFJ	*P*-value
Pitavastatin acid				
C_{max} (ng mL^{-1})	81.4 (22.2, 140.5)	86.0 (42.7, 129.2)	4.6 (−16.9, 26.0)	0.48
t_{max} (h)	0.9 (0.4, 1.3)	1.0 (0.6, 1.4)	0.1 (−0.4, 0.6)	0.58
$t_{1/2}$ (h)	9.0 (7.7, 10.4)	10.1 (7.6, 12.6)	1.1 (−0.8, 2.9)	0.12
AUC_{0-24} (ng mL^{-1} h)	194.2 (104.3, 284.0)	220.1 (149.0, 291.3)	26.0 (−5.0, 56.9)	<0.05
Pitavastatin lactone				
C_{max} (ng mL^{-1})	49.5 (28.9, 70.1)	64.4 (30.6, 98.2)	14.9 (−3.3, 33.1)	0.07
t_{max} (h)	1.6 (1.2, 2.1)	1.6 (0.9, 2.2)	−0.1 (−0.9, 0.7)	0.72
$t_{1/2}$ (h)	6.1 (4.5, 7.7)	9.8 (7.2, 12.3)	3.5 (0.2, 6.8)	<0.05
AUC_{0-24} (ng mL^{-1} h)	269.3 (169.6, 369.1)	351.0 (196.6, 505.5)	81.7 (−4.2, 167.7)	<0.05

GFJ, Grapefruit juice; C_{max}, maximum concentration in plasma; t_{max}, time to maximum plasma concentration; $t_{1/2}$, elimination half-life; AUC_{0-24}, area under the plasma concentration – time curve between time zero and 24 h after dosing.

lowering effect of the statins in hypercholesterolaemic patients [7], and both pathways must be taken into account to avoid potential drug–statin interactions.

In conclusion, repeated intake of GFJ affected the pharmacokinetics of atorvastatin, but had minimal effect on pitavastatin acid. Pitavastatin may be clinically preferable for preventing pharmacokinetic drug-interactions.

No specific funding was received for this study.

References

1 Williams D, Feely J. Pharmacokinetic–pharmacodynamic drug interactions with HMG-CoA reductase inhibitors. Clin Pharmacokinet 2002; 41: 343–70.

2 Kajinami K, Takekoshi N, Saito Y. Pitavastatin efficacy and safety profiles of a novel synthetic HMG-CoA reductase inhibitor. Cardiovasc Drug Rev 2003; 21: 199–215.

3 Fujino H, Yamada I, Shimada S, Yoneda M, Kojima J. Metabolic fate of pitavastatin, a new inhibitor of HMG-CoA reductase: human UDP-glucuronosyltransferase enzymes involved in lactonization. Xenobiotica 2003; 33: 27–41.

4 Guo LQ, Fukuda K, Ohta T, Yamazoe Y. Role of furanocoumarin derivatives on grapefruit juice-mediated inhibition of human CYP3A activity. Drug Metab Dispos 2000; 28: 766–71.

5 Fukazawa I, Uchida N, Uchida E, Yasuhara H. Effects of grapefruit juice on pharmacokinetics of atorvastatin and pravastatin in Japanese. Br J Clin Pharmacol 2004; 57: 448–55.

6 Lilja JJ, Kivisto KT, Neuvonen PJ. Grapefruit juice increases serum concentrations of atorvastatin and has no effect on pravastatin. Clin Pharmacol Ther 1999; 66: 118–27.

7 Kajinami K, Takekoshi N, Brousseau ME, Schaefer EJ. Pharmacogenetics of HMG-CoA reductase inhibitors: exploring the potential for genotype-based individualization of coronary heart disease management. Atherosclerosis 2004; 177: 219–34.

Table I Demographic Characteristics of the Subjects

Age	Height, cm	Weight, kg	Body Mass Index	Gender
33.5 ± 6.4	167.5 ± 5.9	65.9 ± 4.8	23.9 ± 2.9	Male

on day 1 (observation period) at 0800, 1100, 1400, and 2000 hours. Subjects took perindopril erbumine (2 mg of powder plus 98 mg of lactose, wrapped in a wafer), losartan potassium (25 mg of powder plus 75 mg of lactose, wrapped in a wafer), or placebo (100 mg of lactose, wrapped in a wafer) at 0800 hours from days 2 to 15. We have found that these doses do not affect blood pressure after repeated administration in normotensive subjects. On day 15, an evaluation test and samplings of salivary fluid and blood were performed at the same time. On the day of taste evaluation, subjects did not have breakfast, but a similar light meal was served just after the evaluation at 1400 hours. They were prohibited to eat any other food or drink anything except distilled water until the end of the test. After the washout period, an identical protocol was repeated in a crossover fashion. All protocols were approved by the Ethical Committee of Jichi Medical School.

Samplings of Saliva and Blood

Spontaneously salivated salivary fluid was collected after gargling.[6] Serum was transferred into special tubes after centrifugation.[6] All samples were stored at −80°C until the assay. Zinc concentration was measured by atomic absorption spectrophotometry.[8] Plasma renin activity (PRA) was measured by radioimmunoassay.[9]

Evaluation for Taste Disturbance[6]

Semi-Quantitative Clinical Gustometry Using Filter-Paper Disc

Semi-quantitative clinical gustometry using filter-paper discs (Taste Disc, Sanwa Chemical Laboratory, Japan), which is routinely used in clinical settings,[6,10] was performed. In brief, detection thresholds for 4 basic tastes (sweet, salty, sour, and bitter) were evaluated by using the same chemical solutions (sucrose, NaCl, tartaric acid, and quinine, respectively) that were sequentially diluted with distilled water into 5 grades. Concentration number 1 is the lowest, and 5 is the highest (0.3%, 2.5%, 10%, 20%, and 80% for sucrose; 0.3%, 1.25%, 5%, 10%, and 20% for NaCl; 0.02%, 0.2%, 2%, 4%, and 8% for tartaric acid; and 0.001%, 0.02%, 0.1%, 0.5%, and 4% for quinine). Subjects were asked to gargle with distilled water several times just before each test. A small droplet of each solution was added to filter paper (8 mm diameter), which was placed 2 cm on the left side from the tip of the tongue (ie, locus for left chorda tympani nerve) for a second. The test was started from concentration number 1 and gradually increased. The thresholds were determined by the subjects' answers. The order of the test for 4 basic tastes was randomly chosen. Mean thresholds for normal volunteers were less than 3.[10] The test was performed by the same person (S.T.) throughout the study. We have confirmed that the mean changes among 3 continuous examinations were −0.17 ± 0.05, −0.22 ± 0.07, −0.14 ± 0.05, and −0.19 ± 0.05 for sweet, salty, sour, and bitter, respectively, in healthy subjects (n = 8).[6] Thus, we think that the reproducibility of the test was extremely acceptable.

Electrogustometer

The electrogustometry was performed by commercially available equipment (TR-06, Rion Co, Ltd, Tokyo, Japan) as previously described.[6,10] In brief, a single-type stimulation rod was placed on the tongue, as done in the filter-paper disc test, and the electrical stimuli were pulsed from the lowest power (−8 dB) and gradually increased. The smallest stimulus that the subjects noticed was regarded as the threshold. Normal range was less than +14 dB.[10] The test was performed following the filter disc test after gargling with distilled water. The test was performed by the same person (S.T.) throughout the study. We have confirmed that the mean change among 3 continuous examinations was +0.8 ± 0.2 dB in healthy subjects (n = 8).[6] Thus, we think that the reproducibility of the test was extremely acceptable.

Statistics

All data were expressed with mean ± SE. Statistical analysis was performed by analysis of variance. Fisher's protected least significant difference (PLSD) test was used as a post hoc test. $P < .05$ was regarded as significant.

RESULTS

Six subjects completed the protocols, whereas 1 subject dropped out because of a perindopril-induced dry cough. No subject recognized a taste disturbance during the trial. Mean blood pressure just before final dosing was not different among the 3 trials (108 ± 4, 110 ± 5, and 111 ± 5 mm Hg for losartan, perindopril, and placebo, respectively). The recognition threshold of sweetness at the end of the repeated treatment was signifi-

Table II Difference of Area Under the Time-Score Curve of Tests and Time-Concentration Curve of Zinc and Plasma Renin Activity Between Drug and Placebo

	Losartan	Perindopril	Difference of 95% Confidence Interval Between Losartan vs Perindopril
Sweet, unit•h	17.22 ± 4.05	12.20 ± 4.95	(–2.13, 6.42)
Salty, unit•h	13.52 ± 4.31	11.41 ± 3.73	(–2.29, 4.11)
Sour, unit•h	11.06 ± 3.23	8.44 ± 2.69	(–2.99, 3.74)
Bitter, unit•h	20.26 ± 3.95	18.02 ± 3.31	(–3.55, 5.11)
Electrogustometer, dB•h	46.17 ± 8.95	38.37 ± 8.07	(–11.51, 17.17)
Salivary zinc, mg/dL•h	13.79 ± 9.25	–2.81 ± 10.33	(–13.95, 14.21)
Serum zinc, mg/dL•h	2.52 ± 14.75	8.20 ± 15.82	(–12.55, 8.27)
Plasma renin activity, ng/mL	50.8 ± 10.2	45.7 ± 9.4	(–11.2, 17.2)

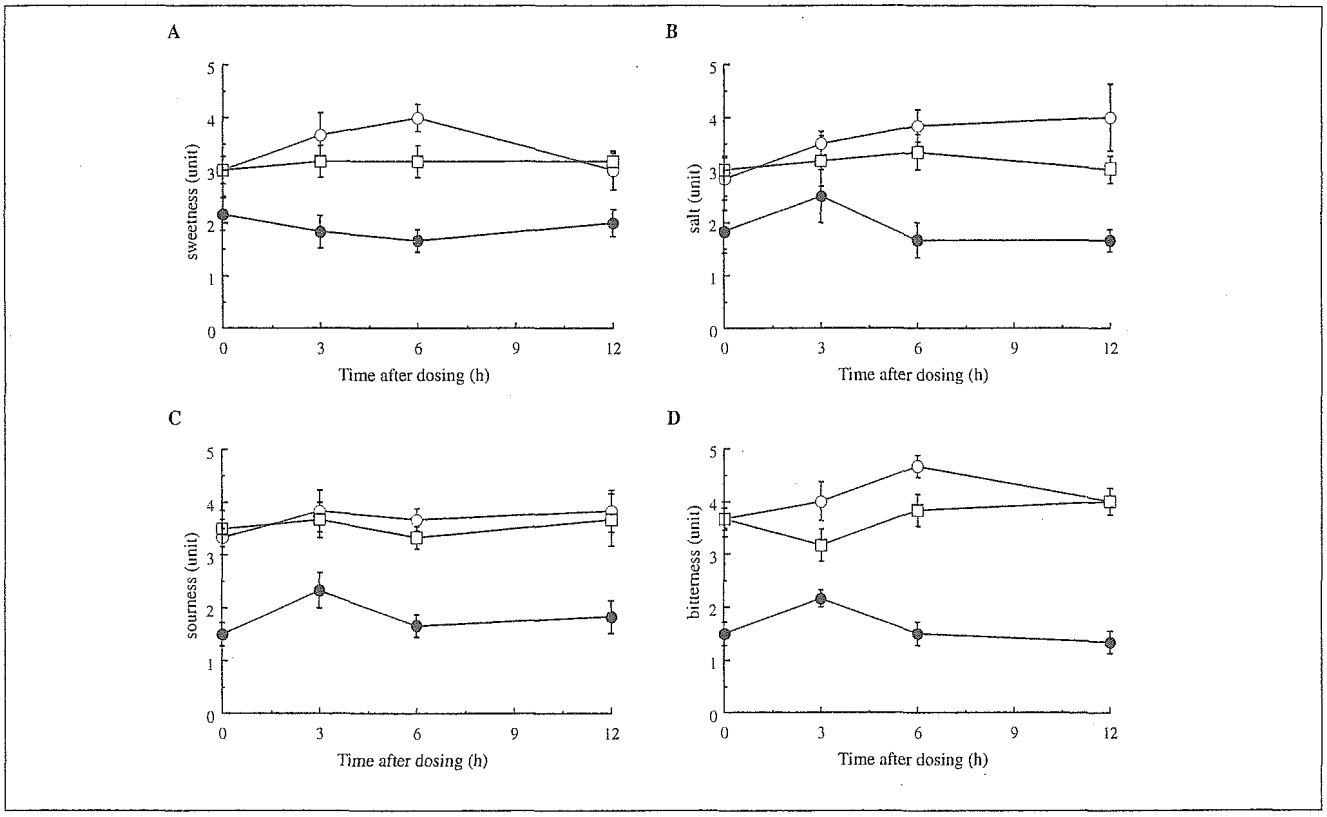

Figure 1. Detection thresholds for tastes using the filter-paper disc after repeated dosing of losartan, perindopril, and placebo. Four basic tastes—sweet (A), salty (B), sour (C), and bitter (D)—were evaluated by using chemical solutions before and at the end of each treatment. A similar test was performed just before each protocol, which confirmed that the disturbances completely disappeared after the washout period (data not shown). Mean ± SE, n = *6. Losartan, open circles; perindopril, open squares; placebo, solid circles.*

cantly worse after treatment with the 2 drugs, whereas the increment of the score was not significantly different between the drugs (Figure 1A). The detection thresholds of the other 3 tastes were also significantly ($P < .05$) worse after repeated treatment with losartan or perindopril but not after placebo (Figure 1B-D). The difference in area under the time-score curve (determined by the trapezoidal method) between drug and placebo is shown in Table II. The decrements of parameters were not different between the 2 drugs. The thresholds of the tastes just before each treatment were not different between the 3 groups (data not shown).

The detection threshold at the end of each trial using an electrogustometer was also worse after losartan or

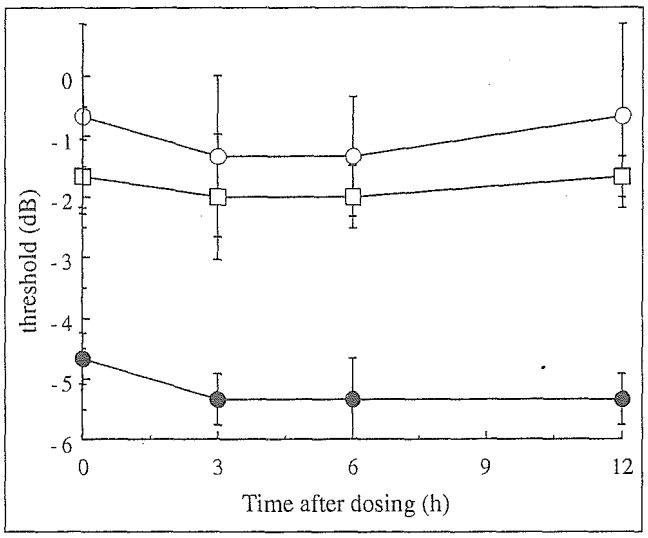

Figure 2. Detection threshold using the electrogustometer after repeated dosing of losartan, perindopril, and placebo. A similar test was performed just before each protocol, which confirmed that the disturbances completely disappeared after the washout period (data not shown). Mean ± SE, n = 6. Losartan, open circles; perindopril, open squares; placebo, filled circles.

perindopril to the same extent but not after placebo (Figure 2). Differences in area under the time-score curve between the drugs and placebo are shown in Table II. The thresholds before each trial were not significantly different among the 3 groups (data not shown).

Salivary and serum zinc concentrations and plasma renin activity at the end of the repeated treatment were measured (Figures 3A,B and 4). Differences in area under the time-concentration curve (determined by the trapezoidal method) between drugs and placebo are shown in Table II. Serum zinc concentration at 12 hours after final dosing was significantly lower than other points in each trial (Figure 3B). Plasma renin activity at the end of the repeated treatment was significantly higher in the trial with losartan and perindopril than with placebo (Figure 4). However, no significant differences between the drug-treated groups were observed in these parameters.

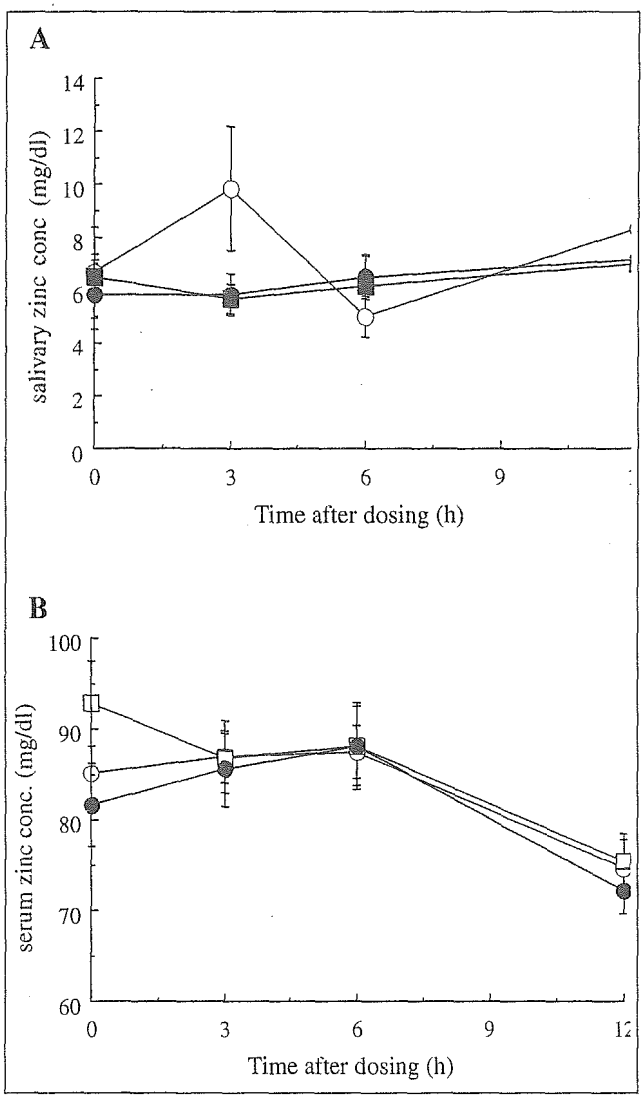

Figure 3. Salivary (A) and serum (B) zinc concentrations before and after repeated dosing of losartan, perindopril, and placebo. Mean ± SE, n = 6. Losartan, open circles; perindopril, open squares; placebo, filled circles.

DISCUSSION

Although drug-induced taste disturbance by ACE inhibitors was well recognized, only 1 case has been reported for perindopril until now.[2] Furthermore, prospective clinical trials on taste were not reported for the drug. This is the first clinical study to show that perindopril subclinically affects taste. Thus, perindopril potentially disturbs taste, which is similar to other ACE inhibitors. Plasma renin activity increased after the drug, but subjects' systemic blood pressure did not decrease, which is compatible with a previous study on perindopril[11] and losartan.[12]

Another important issue in this study is that we directly compared the effect of losartan, an ARB, and perindopril, an ACE inhibitor, on taste sensitivity in healthy subjects with a crossover study and determined their effects. We found that the taste disturbance by the 2 drugs at the dosages used was similar in quality and quantity. It was recently reported that coadministration of ARB and ACE inhibitors has beneficial effects on the preservation of renal function in patients with chronic renal insufficiency.[7] This study indicates

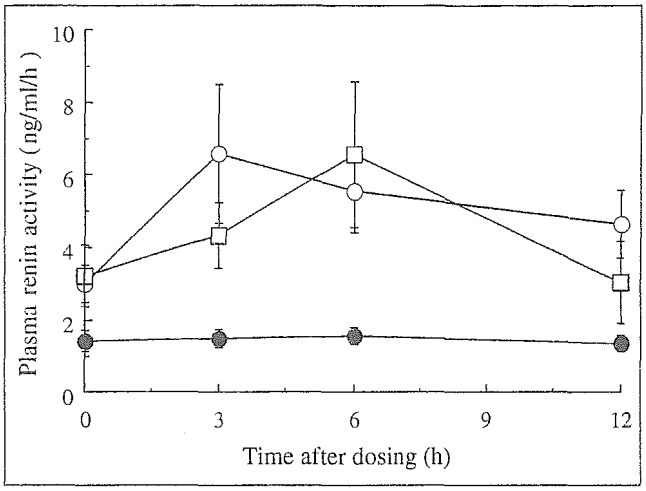

Figure 4. Plasma renin activity at the end of each treatment. Mean ± SE, n = 6. Losartan, open circles; perindopril, open squares; placebo, filled circles.

that coadministration of ARB and ACE inhibitors might additively worsen taste. Careful monitoring is needed in this clinical situation.

The mechanisms of the taste disturbances by these drugs remain uncertain. These drugs similarly increased plasma renin activity but did not affect serum and salivary zinc concentrations. Thus, alteration of the renin-angiotensin-system might directly or indirectly affect the taste sensation system. Perindopril causes taste disturbance and possesses strong tissue ACE affinity among ACE inhibitors.[13] In addition, other ACE inhibitors that possess less affinity to tissue ACE are reported to cause taste disturbances in clinical practice.[1-3] These observations indicate that taste disturbance does not depend on tissue ACE activity. Further studies are needed to evaluate the mechanisms.

The number of subjects who participated in this study was small, which is a major limitation. We could detect the subclinical taste disturbance by the drug in this small population; therefore, the number of patients who have similar subclinical disorders must be very large in the clinical situation. If hypertensive patients with slight taste disturbance receive these drugs, the drug-induced taste disturbance might be clinically obvious.

In this study, drug-induced taste disturbances seemed to be larger for "bitterness" and "sourness" than "salt" and "sweetness." Recent advances in molecular biology have identified some receptors and ion channels on taste cells. Sweet and bitter tastes are mediated by large families of taste receptors, which are G-protein-coupled proteins with 7 transmembrane domains.[14,15] On the other hand, salt and sour tastes are elicited by some ion channels (salt, amiloride-sensitive epithelial Na channel; sour, amiloride-sensitive epithelial Na channels and H^+-activated cation channels).[14,15] Our results indicate that deteriorating effects of perindopril and losartan on taste depend on these receptors/channels. Further studies with a larger number of subjects are needed to evaluate the precise mechanisms.

In conclusion, we compared the effect of losartan and perindopril on taste in healthy Japanese male volunteers. Both drugs subclinically worsened taste to a similar extent in quality and quantity. Careful monitoring is necessary, especially in the case of coadministration.

REFERENCES

1. Henkin RI. Drug-induced taste and smell disorders: incidence, mechanisms and management related primarily to treatment of sensory receptor dysfunction. *Drug Safety.* 1994;11:318-377.

2. Tomita H, Yoshikawa T. Drug-related taste disturbances. *Acta Otolaryngol Suppl.* 2002;546:116-121.

3. Heyneman CA. Zinc deficiency and taste disorders. *Ann Pharmacother.* 1996;30:186-187.

4. Schlienger RG, Saxer M, Haefeli WE. Reversible ageusia associated with losartan. *Lancet.* 1996;347:471-472.

5. Heeringa M, van Puijenbroek EP. Reversible dysgeusia attributed to losartan. *Ann Intern Med.* 1998;129:72.

6. Tsuruoka S, Wakaumi M, Nishiki K, et al. Subclinical alteration of taste sensitivity induced by candesartan in healthy subjects. *Br J Clin Pharmacol.* 2004;57:807-812.

7. Andersen NH, Mogensen CE. Dual blockade of the renin angiotensin system in diabetic and nondiabetic kidney disease. *Curr Hypertens Rep.* 2004;6:369-376.

8. Meret S, Henkin R. Simultaneous direct estimation by atomic absorption spectrophotometry of copper and zinc in serum, urine, and cerebrospinal fluid. *Clin Chem.* 1971;17:369-373.

9. Heise C. Measurement of plasma renin activity. *Clin Chem.* 1975;21:447-449.

10. Tomita H, Ikeda M, Okuda Y. Basis and practice of clinical taste examinations. *Auris Nasus Larynx.* 1986;13(suppl 1):S1-S15.

11. Lees KR, Reid JL. Haemodynamic and humoral effects of oral perindopril, an angiotensin converting enzyme inhibitor, in man. *Br J Clin Pharmacol.* 1987;23:159-164.

12. Ohtawa M, Takayama F, Saitoh K, Yoshinaga T, Nakashima M. Pharmacokinetics and biochemical efficacy after single and multiple oral administration of losartan, an orally active nonpeptide angiotensin II receptor antagonist, in humans. *Br J Clin Pharmacol.* 1993; 35:290-297.

13. Takai S, Jin D, Sakaguchi M, Miyazaki M. Significant target organs for hypertension and cardiac hypertrophy by angiotensin-converting enzyme inhibitors. *Hypertens Res.* 2004;27:213-219.

14. Gilbertson T, Damak S, Margolskee R. The molecular physiology of taste transduction. *Curr Opin Neurobiol.* 2000;10:519-527.

15. Lindemann B. Receptors and transduction in taste. *Nature (Lond).* 2001;413:219-225.

Clinical and Experimental Pharmacology and Physiology (2005) **32**, 1034–1041

ACUTE DIGOXIN LOADING REDUCES ABCA8A mRNA EXPRESSION IN THE MOUSE LIVER

Michi Wakaumi,*† Kenichi Ishibashi,‡ Hitoshi Ando,* Hiroshi Kasanuki† and Shuichi Tsuruoka*

**Department of Pharmacology, Division of Clinical Pharmacology, Jichi Medical School, Tochigi, †Department of Cardiology, Tokyo Women's Medical University, Tokyo and ‡Division of Molecular Biology Research, Clinical Research Center, Chiba-East National Hospital, Chiba, Japan*

SUMMARY

1. Human ABCA8, a new member of the ATP binding cassette (ABC) transporter family, transports certain lipophilic drugs, such as digoxin. To investigate the roles of this transporter, we cloned a mouse homologue of ABCA8, from a mouse heart cDNA library, named ABCA8a.

2. The deduced mouse ABCA8a protein is 66% identical with that of human ABCA8 and possesses features common to the ABC superfamily. It was found that ABCA8a was mainly expressed in the liver and heart, similar to human ABCA8.

3. We further evaluated the effect of acute digoxin (a substrate for ABCA8) intoxication on the mRNA expression of ABCA8 using northern blotting with a 3′ non-coding region as a probe to avoid cross-hybridization with other ABCA genes.

4. Following acute digoxin infusion, the mRNA expression of ABCA8 was significantly reduced in the liver 12–24 h after injection (14.7% of vehicle treatment), but not in the heart and kidney.

5. Real-time quantitative polymerase chain reaction analysis confirmed the reduction in ABCA8a mRNA. Similar reductions in ABCA5, ABCA7, ABCA8b and ABCA9 mRNA were also observed. A comparable amount of digitoxin did not affect ABCA8a mRNA expression in the liver.

6. The results suggest that ABCA8 may play a role in digoxin metabolism in the liver.

Key words: ATP binding cassette (ABC) transporter, cloning, digoxin intoxication, mouse, mRNA.

INTRODUCTION

The ATP binding cassette (ABC) superfamily consists of more than 400 proteins and is widely distributed in nature from bacteria to human.[1] We have reported previously that human ABCA8, a new member of the ABC-A family, is a drug transporter for lipophilic drugs (such as digoxin and glucuronide conjugates).[2] However, the physiological and pathophysiological roles of this protein are not known at present. Currently, human ABC-A family has 13 genes (*ABCA1–ABCA13*). Because *ABCA11* is a pseudogene, 12 members of the ABC-A family are present in the human body. These genes are divided into two subfamilies. The ABCA1–A4, ABCA7, ABCA12 and ABCA13 genes are relatively homologous with each other (approximately 50%) and have been grouped as one subfamily. Recently, some of these genes have been found to be the cause of genetic diseases: ABCA1, ABCA4 and ABCA12 have been identified as the genes responsible for Tangier disease,[3] Stargardt disease[4] and a skin disease known as lamellar ichthyosis type 2,[5] respectively. All three conditions are thought to be caused by a dysfunction in cholesterol transport into cells. The members of the other subfamily (ABCA5–6, ABCA8–10) have a higher homology with each other (60–70%) and all are localized at the same locus, chromosome 17q24.[1,2] These genes may derive from local gene duplications. Currently, however, their roles and related diseases are unknown. Our previous report on the function of ABCA8 is the only published report so far documenting its function.[2]

To address the physiological and pathophysiological roles of ABCA8, in the present paper we first cloned a mouse *ABCA8* gene. Because digoxin is a substrate for this transporter, we speculated that the mRNA expression of the *ABCA8* gene would be affected under conditions of digoxin intoxication, which is sometimes observed in the clinical situation.[6] Therefore, we next made a mouse model of digoxin intoxication and examined the mRNA expression of *ABCA8* in three organs, namely the heart as the target organ and the kidney and liver as metabolising organs. We also compared the effect of digitoxin, another cardiac glycoside with different pharmacokinetics to digoxin, on the mRNA expression of *ABCA8*.

METHODS

Identification of mouse *ABCA8a* cDNA and the 3′ non-coding region

A mouse ABCA8 homologue was searched for in a mouse heart cDNA library (Mouse Heart 5′-STRECH PLUS cDNA®; Clontech, Palo Alto, CA, USA) by hybridization with human ABCA8 cDNA[2] (NCBI Accession no. NM_007168) as a probe in 40% formamide, 25% of 20× standard sodium phosphate EDTA (SSPE), 1× Denhart, 0.2% sodium dodecyl sulphate (SDS) and 0.1 mg/mL salmon sperm DNA at 42°C for 16 h and thereafter by washing in 2× standard saline citrate (SSC) for 30 min at room temperature.[7] Because only a partial cDNA was obtained, we further

Correspondence: Dr Shuichi Tsuruoka, Department of Pharmacology, Division of Clinical Pharmacology, Jichi Medical School, 3311 Yakushiji, Minamikawachi, Kawachi, Tochigi 329-0498, Japan.
Email: tsuru@jichi.ac.jp

Received 11 May 2005; revision 21 June 2005; accepted 26 June 2005.

performed 5′ rapid amplification of cDNA ends (RACE; Mouse Heart Marathon-Ready cDNA; Clontech) to obtain a full-length clone. The sequence was examined using a sequence analyser (373-S; PerkinElmer, Fremont, CA USA).[7]

Northern blot analysis of mouse ABCA8a

A transferred filter with mouse total RNA (2 μg poly A + RNA was loaded in each lane) from various organs (heart, brain, spleen, lung, liver, skeletal muscle, kidney and testis) was purchased in the Mouse 8-lane MTN Blot kit (Clontech). The filter was hybridized for 3 h at 68°C in hybridization solution (ExpressHyb; Clontech) with a probe of mouse Abca8a cDNA-3′ uncoding sequence to avoid cross-hybridization with other homologues or with a probe of full-length human glyceraldehyde-3-phosphate dehydrogenase (*GAPDH*) cDNA. Both probes were labelled with [α-^{32}P]-dCTP by random priming. The filter was finally washed in 0.2× SSC and 0.1% SDS at 58°C for 30 min and then exposed to X-ray film at −70°C between two intensifying screens. Densitometric analysis was performed with computer software (Scion Image; Scion, Frederick, MD, USA).

Animal preparation for digoxin intoxication

Male C57BL/6J mice (18–24 g; $n = 62$) were purchased from Japan Clea (Tokyo, Japan) and kept under conditions of free access to standard mouse chow and distilled water. Single dosing of digoxin (2.5 and 0.25 μg/g bodyweight as high and low doses, respectively) or vehicle (ethanol 86 mg/mL, propylene glycol 208 mg/mL and benzyl alcohol 21 mg/mL) was performed by intraperitoneal (i.p.) injections of the substances (0.01 mL/g bodyweight) into mice to establish an acute digoxin-intoxicated model. Mice were anaesthetized by ether at 8, 12, 16, 24 and 48 h after i.p. injection and the heart, liver and kidney were removed. Total RNA was extracted using the RNeasy Mini kit (QIAGEN Sciences, Valencia, MD, USA) and electrophoresed on 1% agarose gels. The RNA was transferred to Hybond-N nylon membranes (Amersham, Braunschweig, Germany) by capillary transfer. The filters used for northern blot analysis were treated according to the same procedures as those used for the determination of tissue distribution described above. All values were corrected by those for GAPDH for loading and transfer differences.

For measurements of serum digoxin concentrations, arterial blood was obtained from each mouse by puncture of the left ventricle. The digoxin concentration was determined using a monoclonal polarization immunoassay technique (TDx autoanalyser; Dinabot, Osaka, Japan.).[8] All experimental protocols were approved by the Committee for Animal Research/Genetic Research of Jichi Medical School.

Real-time quantitative polymerase chain reaction

Reverse transcription was performed with 1.2 μg total RNA, random hexamer primers and RevertAid M-MuLV reverse transcriptase (Fermentas, Hanover, MD, USA).[9] The resulting cDNA, equivalent to 60 ng RNA, was used for real-time quantitative polymerase chain reaction (PCR) in an ABI Prism 7700 sequence detection system (Applied Biosystems, Foster City, CA, USA). All specific sets of primers and TaqMan probes used in the present study were obtained from Applied Biosystems (Assays-on-Demand Gene Expression Products and TaqMan Rodent GAPDH Control Reagants). All primer sets, with the exception of TaqMan Rodent GAPDH Control Reagants, were designed to be located in two exons to avoid amplification of potentially contaminating genomic DNA. To control for the variation in the amount of DNA available for PCR in the different samples, gene expressions of the target sequence were normalized in relation to the expression of the endogenous control GAPDH. In the present study, no agent affected the mRNA expression of GAPDH: the coefficients of variation of its threshold cycle (Ct) values were all < 3%. Because the efficiency of target amplification was approximately equal to that of GAPDH amplification, data were analysed using the comparative threshold cycle method.[10] Because the intra- and interassay coefficients of variation of the relative expression values were < 20%, we considered mean relative values of less than 0.8 or more than 1.2 to be significant in the present study.[9]

Statistics

Data are expressed as the mean±SEM. Statistical analysis was performed using non-paired *t*-test with StatView computer software (SAS, Cary, NC, USA). $P < 0.05$ was considered significant.

RESULTS

Identification and tissue distribution of mouse *ABCA8a* mRNA

We cloned a total of 5542 nucleotides of cDNA, which contained the full-length of mouse *ABCA8a* cDNA with a 4863 bp open reading frame (ORF). This sequence has been deposited at GenBank (Accession no. AY732492). The C-terminus has a poly A tail with a polyadenylation signal (AATAAA) upstream. The deduced amino acid sequence possesses two ATP-binding cassettes and Walker A motifs, both of which are highly conserved in all ABC superfamilies (Fig. 1). The mouse ABCA8a protein was 66% identical with human ABCA8 protein at the amino acid level (Fig. 2). While the present study was being undertaken, the entire mouse genome was sequenced[11] and the full-length mouse *ABCA8a* cDNA was registered at GenBank (Accession no. NM_153145). However, the 3′ non-coding sequence is incomplete.

Because the sequence of the *ABCA8a* gene is highly homologous with that of other ABCA group genes (*ABCA5*,[12] *ABCA6*,[13] *ABCA9*,[14] *ABCA10*[15] and, in particular, *ABCA8b*), the non-coding region of the 3′-end of the gene (nucleotide no. 4969–5480, 512 bp; see Fig. 1) was chosen for as a probe in northern blot analysis to avoid cross-hybridization with other ABCA genes. Figure 3 shows the expression of *ABCA8a* mRNA in various mouse tissues. The size of the transcript was approximately 6.5 kb, suggesting that our cDNA is devoid of a 5′ non-coding sequence (approximately 1 kb). Expression was prominent in the liver and heart and faint in the kidney, lung and skeletal muscle; expression was not observed in the brain, spleen and testis. Similar results were obtained using full-length *ABCA8a* cDNA as a probe (data not shown). Therefore, in retrospect, cross-hybridizations did not pose much of a problem.

Effect of acute digoxin intoxication on *ABCA8a* mRNA expression in the liver, heart and kidney

We injected a single bolus of digoxin to produce an acute digoxin intoxication mouse model, in which two doses of digoxin were used. Although both doses were expected to be toxic to the mouse, all mice survived until tissue retrieval. Figure 4 shows the time-course of mRNA expression in the liver, heart and kidney following injection of the higher dose of 2.5 μg/g bodyweight digoxin. The mRNA expression in the liver decreased from 12 to 24 h after digoxin injection (Figs 4a,5). The reduction in mRNA expression was most prominent 24 h after the injection and was completely recovered 48 h after the injection. The mRNA expression in the heart and kidney was not affected by digoxin injection (Fig. 4b,c). The expression of *GAPDH*, a house-keeping gene, was not altered

by the digoxin injection (data not shown). The reduction of the *ABCA8a* mRNA expression in the liver at 24 h after injection was further confirmed by real-time quantitative reverse transcription–PCR (RT-PCR; Fig. 6). The relative expression of *ABCA8a* mRNA

was 1.19 ± 0.24 and 0.15 ± 0.03 following injection of vehicle and digoxin, respectively ($P < 0.01$). We also evaluated the effect of a lower dose of digoxin on mRNA expression of *ABCA8a* in the liver 24 h after injection. As shown in Fig. 7, 0.25 μg/g bodyweight digoxin did not change the mRNA expression of *ABCA8a*. The serum digoxin concentration 24 h after injection of 2.5 and 0.25 μg/g bodyweight digoxin was 100.1 ± 10.9 and 4.7 ± 2.9 ng/mL ($n = 6$ in each group), respectively. Therefore, higher blood levels of digoxin are necessary to alter *ABCA8a* mRNA expression.

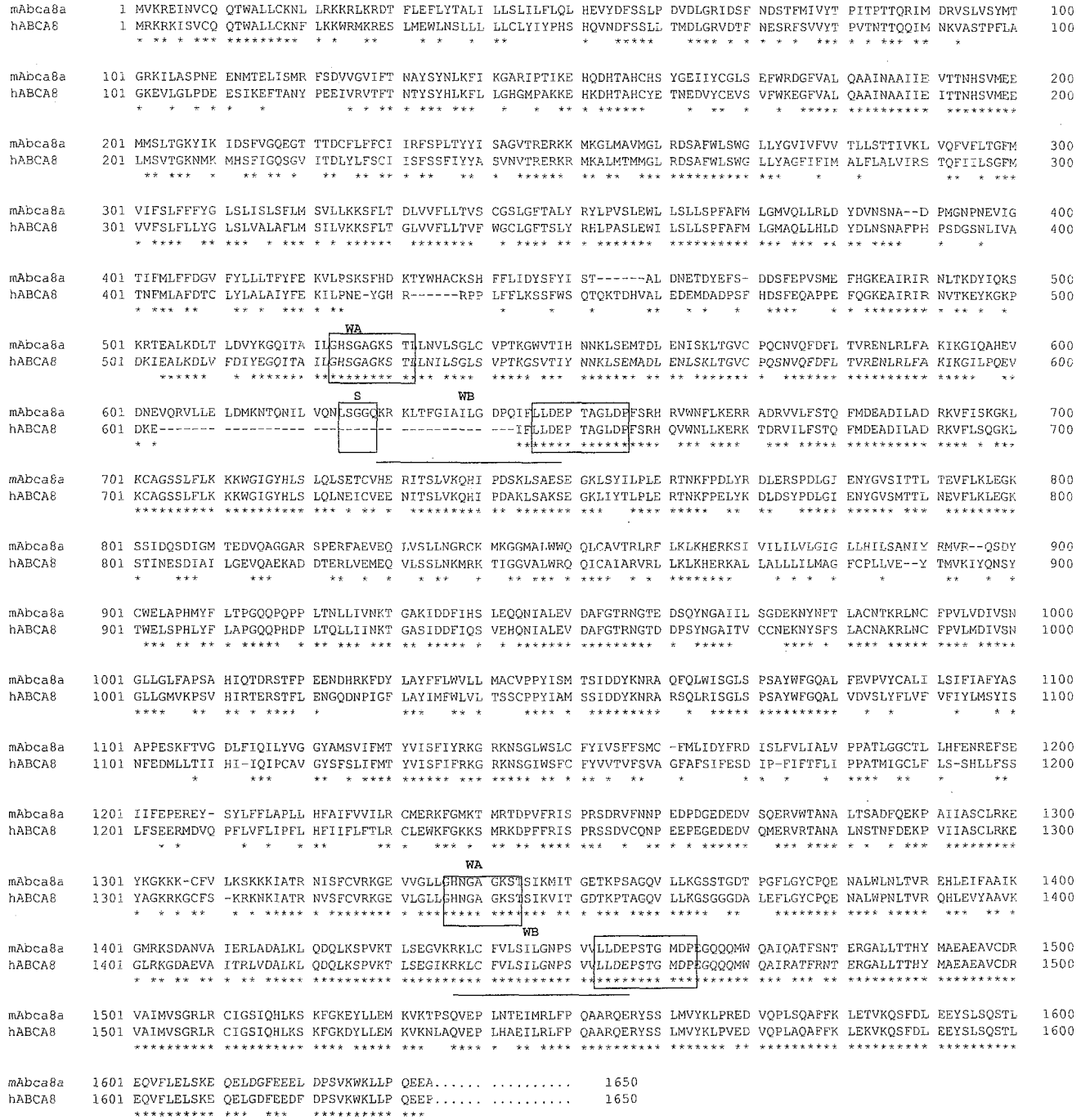

Fig. 2 *Amino acid sequence alignment of the mouse ABCA8a (mAbca8a) with human ABCA8 (hABCA8) performed using CLUSTALW (http://www.ebi.ac.uk/clustalw). Sequences that are identical between the two are marked with asterisks (*) and sequence gaps introduced by best-fit alignment are shown by underlining. Prominently conserved sequences of the ATP binding cassette (ABC) regions are framed. WA, Walker A motif; S, ABC family signature sequence. The genuine Walker B motif is underlined.*

Fig. 1 *Nucleotide sequence alignment of mouse ABCA8a with mouse ABCA8b and mouse ABCA9 performed with CLUSTALW (http://www.ebi.ac.uk/clustalw). Sequences that are identical among three the ABCA genes are marked with asterisks (*) and sequence gaps introduced by best-fit alignment are shown by underining. The nucleotide sequence of the 3′ end of the non-coding region of mouse ABCA8a, used as the probe for northern blot (nucleotide no. 4969–5480, 512 bp), is framed. The mouse ABCA8a sequence was registered at GenBank under Accession no. AY732492.*

Because the cellular effect of cardiac glycosides may lead to a reduction in *ABCA8a* mRNA expression, the effect of another cardiac glycoside, namely digitoxin, was evaluated. As shown in Fig. 8, injection of a comparable amount of digitoxin (0.25 and 2.5 μg/g bodyweight; the molecular weights of digitoxin and digoxin are similar, being 764.9 and 780.9, respectively) did not affect *ABCA8a* mRNA expression. Therefore, the effect of digoxin on *ABCA8a* mRNA expression was not caused by the cellular effect of the cardiac glycoside. Finally, we evaluated the change in mRNA expression of *ABCA5*, *ABCA7*, *ABCA8b* and *ABCA9* after acute digoxin loading in mouse livers using real-time quantitive RT-PCR. As shown in Fig. 9, the mRNA expression of these genes was also significantly decreased, although the magnitudes of the effect on the mRNA expression of *ABCA5*, *ABCA7* and *ABCA9* was less pronounced than that on the mRNA expression of *ABCA8a*. Therefore, the *ABCA8a* gene is not the only gene affected by digoxin. Other members of this subfamily are similarly affected by digoxin treatment.

DISCUSSION

In the present study, we cloned a mouse *ABCA8a* cDNA containing the full ORF. We found that the mouse *ABCA8a* gene was highly similar (66% identity at the amino acid level) to human *ABCA8* and that they shared common features of the ABC superfamily. We also found that *ABCA8a* cDNA was relatively similar to other ABC-A members, especially *ABCA8b* and *ABCA9* with approximately 73 and 70% identity at the nucleotide levels, respectively.[14] Table 1 summarizes the available published information on *ABCA5*, *ABCA6*, *ABCA8*, *ABCA9* and *ABCA10* genes. Interestingly, these genes are localized in the vicinity of the same chromosomal locus and their tissue distributions partly overlap. In the present study, mRNA expression of *ABCA8a* was prominent in the heart and liver, which indicates that the tissue distribution of ABCA8a in the mouse is similar to that of human ABCA8. Of note, the mouse has two homologues of human ABCA8 and both are too close to determine which is the orthologue of human ABCA8. The two homologues may arise from local gene duplication unique to rodents. Alternatively, one of the human counterparts has been lost or has not yet been found. Further analyses of the orders of chromosomal localization, promoter sequences, tissue distributions, transporter functions and regulation of expression will be necessary to determine which is the mouse orthologue of human *ABCA8*.

To obtain an insight into the pathophysiological roles of ABCA8, we examined ABCA8a expression in an animal model of acute digoxin intoxication, because we have found previously that digoxin is one of the substrates for human ABCA8 protein.[2] We observed a significant reduction in *ABCA8* mRNA in the liver from 12 to 24 h and recovery of mRNA expression 48 h after injection

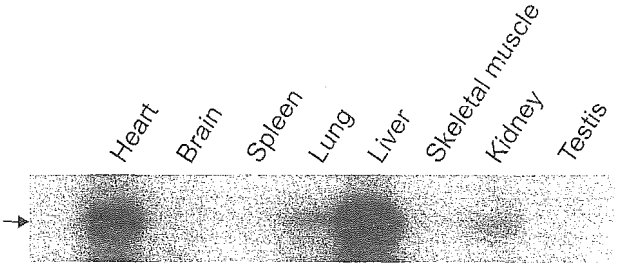

Fig. 3 Northern blot analysis of mouse tissues. A mouse 8-Lane MTN Blot (Clontech, Palo Alto, CA, USA) was hybridized with a probe of a 3′ non-coding sequence of mouse Abca8a cDNA shown in Fig. 1. Poly A+ RNA (2 μg) was loaded in each lane. Expression was prominent in the liver and heart and faint in the kidney and lung. A single band at approximately 6.5 kb (arrow) was observed.

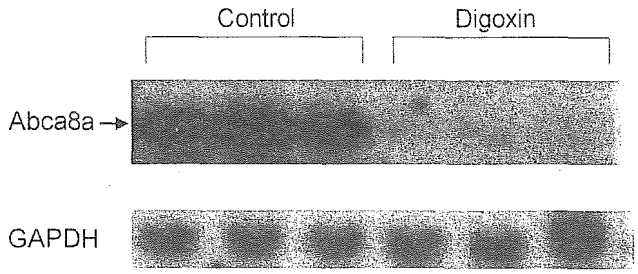

Fig. 5 Representative photo of northern blot analysis in the liver 24 h after injection of 2.5 μg/g bodyweight digoxin. GAPDH was used as the housekeeping gene.

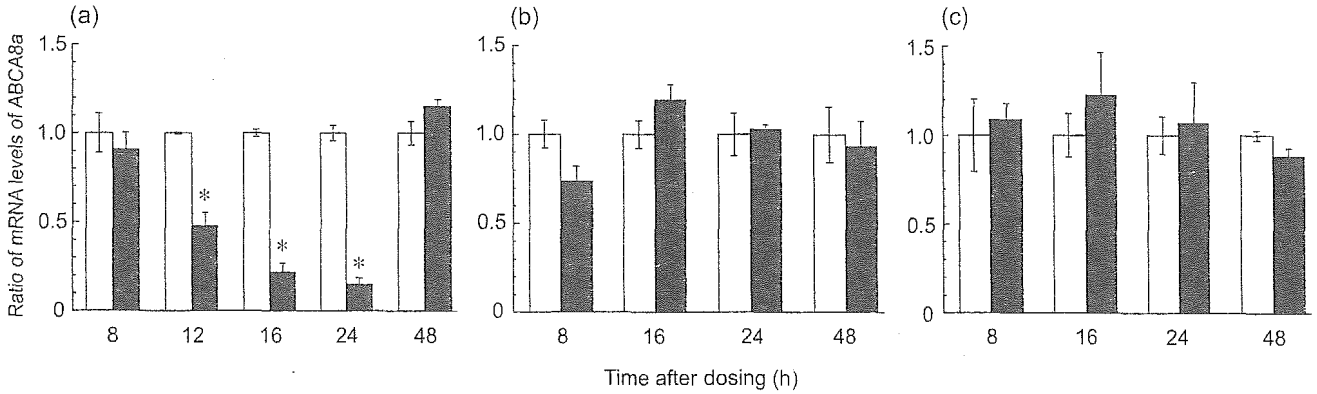

Fig. 4 Time-course of mouse ABCA8a mRNA expression detected by northern blot analysis in the liver (a), heart (b) and kidney (b) following injection of 2.5 μg/g bodyweight digoxin (■). Treatment with vehicle (□) served as a time control. All values were corrected for by those of GAPDH for loading and transfer differences. The mRNA expression of *ABCA8a* in the liver decreased from 12 to 24 h after digoxin injection. The reduction was most prominent at 24 h after injection and was completely recovered 48 h after the injection. Data are the mean±SEM (n = 4–8 for each time point). *P < 0.05 compared with vehicle.